Dynamics and retention of misfolded proteins in native ER membranes

Sarah Nehls*, Erik L. Snapp*, Nelson B. Cole*, Kristien J.M. Zaal*, Anne K. Kenworthy*, Theresa H. Roberts*, Jan Ellenberg†, John F. Presley*, Eric Siggia‡ and Jennifer Lippincott-Schwartz*§

*Cell Biology and Metabolism Branch, National Institute of Child Health and Human Development, Building 18T, National Institute of Health, Bethesda, Maryland 20892, USA

†Gene Expression and Cell Biology Program, European Molecular Biology Laboratory, Heidelberg, Germany

‡Center for Studies in Physics and Biology, Rockefeller University, New York, New York 10021, USA

§e-mail: jlippin@helix.nih.gov

When co-translationally inserted into endoplasmic reticulum (ER) membranes, newly synthesized proteins encounter the lumenal environment of the ER, which contains chaperone proteins that facilitate the folding reactions necessary for protein oligomerization, maturation and export from the ER. Here we show, using a temperature-sensitive variant of vesicular stomatitis virus G protein tagged with green fluorescent protein (VSVG–GFP), and fluorescence recovery after photobleaching (FRAP), the dynamics of association of folded and misfolded VSVG complexes with ER chaperones. We also investigate the potential mechanisms underlying protein retention in the ER. Misfolded VSVG–GFP complexes at 40 °C are highly mobile in ER membranes and do not reside in post-ER compartments, indicating that they are not retained in the ER by immobilization or retrieval mechanisms. These complexes are immobilized in ATP-depleted or tunicamycin-treated cells, in which VSVG–chaperone interactions are no longer dynamic. These results provide insight into the mechanisms of protein retention in the ER and the dynamics of protein-folding complexes in native ER membranes.

A model system for studying pathways for protein folding and misfolding in the ER and their effects on the retention and export of ER proteins is provided by the temperature-sensitive ts045 variant of VSVG, which contains a single lumenal amino-acid change that leads to misfolding and retention within the ER at 40 °C[1–4]. Upon shifting to 32 °C, misfolding is reversed; VSVG then correctly folds and is exported from the ER for delivery to the plasma membrane. Correct folding of VSVG in the ER requires the formation of intrachain disulphide bonds and involves interactions with the folding enzyme protein disulphide isomerase (PDI) and two chaperones, the ATPase BiP (GRP78) and calnexin[5–8]. The chaperone interactions promote the formation of a mature, transport-competent form of VSVG that exists as an oxidized (disulphide-bonded), noncovalently associated homotrimer containing two *N*-linked sugar chains[7,9].

Biochemical analyses have shown that when misfolded VSVG is retained in the ER at 40 °C, complexes of VSVG–BiP and VSVG–calnexin are formed[6–8], although the size, organization and dynamics of these complexes in native ER membranes are not known. This has made it difficult to distinguish between different models for retention of VSVG in the ER at 40 °C, which include: immobilization or aggregation of VSVG–chaperone complexes in ER membranes; failure of VSVG complexes to be recognized by ER export machinery; and continuous retrieval of misfolded VSVG complexes from a post-ER compartment[10,11].

Here we distinguish between these models of ER retention and investigate the dynamics of VSVG–chaperone interactions by measuring the diffusional mobility of folded and misfolded forms of VSVG–GFP[3] that are localized in the ER. The diffusional mobility of VSVG–GFP was quantified using FRAP, in which fluorescent proteins in a small area are irreversibly photobleached by an intense laser flash and fluorescence recovery through the exchange of bleached for nonbleached protein is measured using an attenuated laser beam[12]. Mobility parameters, including the diffusion coefficient, *D*, and the mobile fraction, can be derived from the kinetics of fluorescence recovery to provide insight into the dynamics of VSVG–GFP complexes. For example, if misfolded VSVG molecules are associated with slowly diffusing ER proteins, form large aggregates, or are present in a protein-dense environment, then their apparent *D* value will be lower than for proteins freely diffusing in a lipid bilayer. Alternatively, if they associate irreversibly with immobile ER components or segregate into membrane subdomains, their observed mobile fraction value will be low.

Our results, obtained using FRAP and repetitive photobleaching techniques, show that both folded and misfolded forms of VSVG–GFP are completely mobile in ER membranes, have a diffusion coefficient close to the theoretical limit for protein diffusion in a lipid

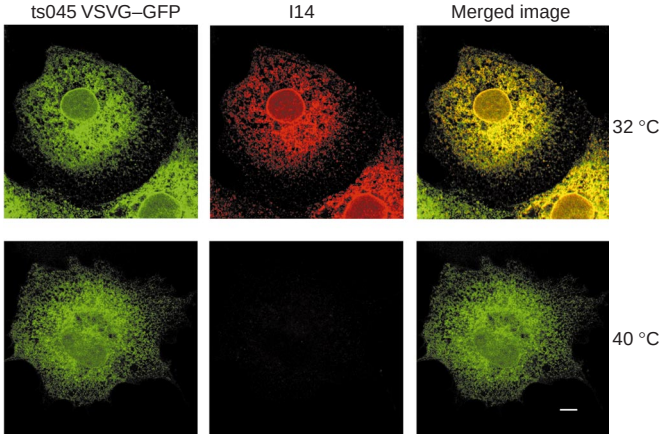

Figure 1 **Attachment of GFP to ts045 VSVG does not alter its temperature-dependent folding.** Cells transfected with VSVG–GFP were incubated for 24 h at 40 °C or at 32 °C in the presence of brefeldin A, which blocks ER export of proteins[16]. Cells were then fixed and stained with the conformation-specific monoclonal antibody I14 to identify correctly folded forms of VSVG–GFP. In cells incubated at 32 °C (upper panels), correctly folded VSVG–GFP retained in the ER was recognized by the I14 antibody, as shown by the complete overlap of antibody staining and distribution of the chimaera. In cells incubated at 40 °C (lower panels), VSVG–GFP was not recognized by the I14 antibody, indicating that it is misfolded in the ER at this temperature. Scale bar represents 10 μm.

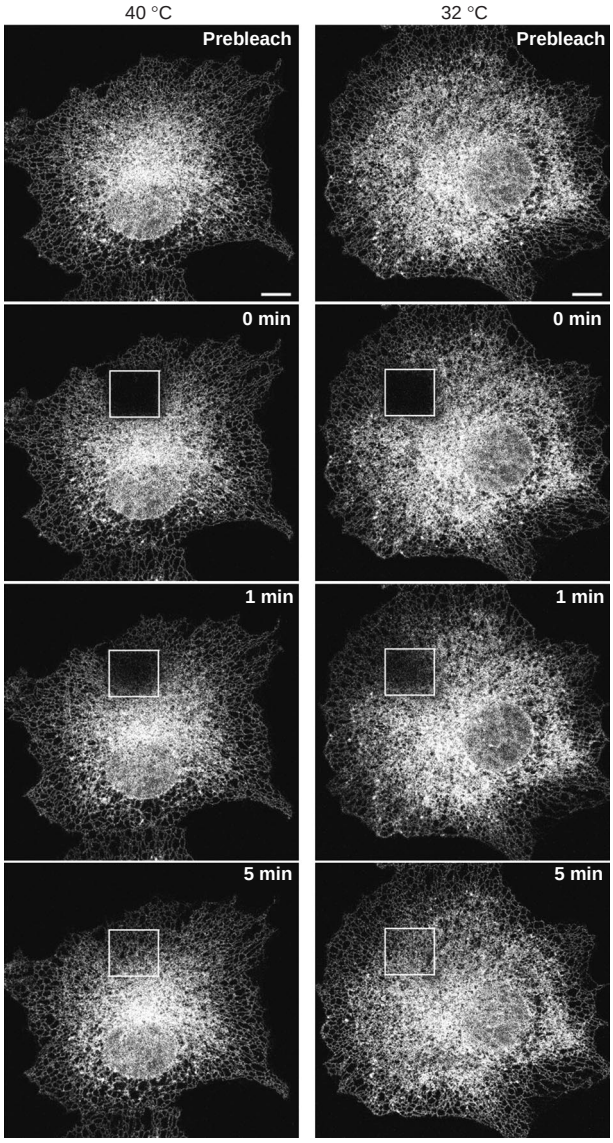

Figure 2 **Both correctly folded (32 °C) and misfolded (40 °C) forms of VSVG–GFP are highly mobile in ER membranes.** Qualitative FRAP analysis of ER-localized VSVG–GFP in cells incubated at 40 °C or 32 °C in the presence of brefeldin A for 24 h. Images were obtained before photobleaching and at the indicated time points after. The photobleached area is outlined by a box. Scale bars represent 10 μm.

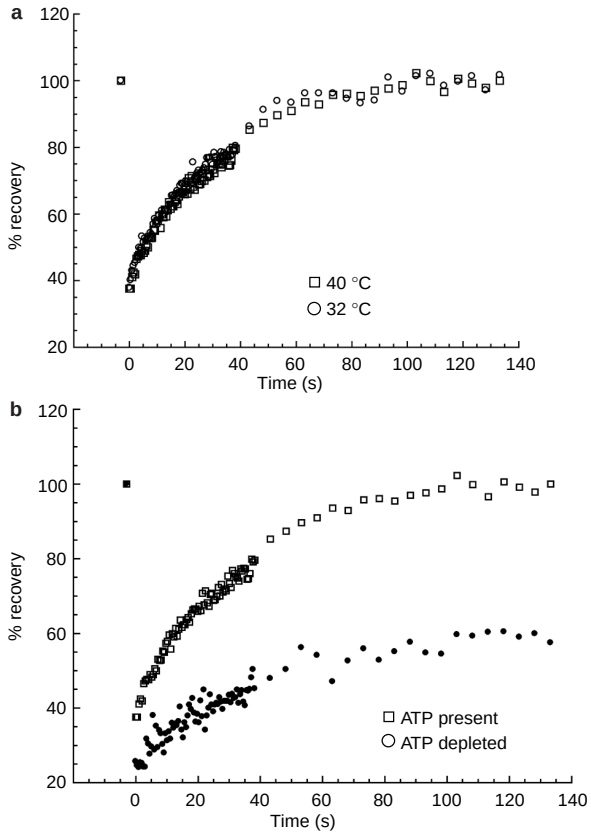

Figure 3 **The extent and time course of fluorescence recovery for VSVG–GFP in the ER are similar at 32 °C and 40 °C, but are decreased by ATP depletion.** Fluorescence intensities (normalized to prebleach values) from FRAP analyses were plotted against time for VSVG–GFP in the ER at 40 °C or 32 °C in the presence of brefeldin A (**a**), and for VSVG–GFP in the ER at 40 °C with or without ATP depletion (sodium azide and 2-deoxy-glucose in glucose-free medium for 15 min) (**b**). Measurements were taken at 0.5-s intervals until a plateau was reached.

bilayer and do not reside in separate ER subdomains or post-ER compartments. This implies that misfolded VSVG complexes are not normally tethered to an underlying ER scaffold or immobilized within a matrix of aggregated proteins, and that they are not retrieved from post-ER compartments. Our data thus support the idea that retention of misfolded VSVG molecules in the ER at 40 °C occurs predominantly as a result of the failure of these proteins to be recognized by ER export machinery. In conditions in which VSVG–chaperone interactions become irreversible and extensive, including ATP depletion and tunicamycin treatment[7,13,14], VSVG–GFP molecules are immobilized and the diffusional mobility of soluble ER proteins is altered. These results indicate that when interactions between misfolded proteins and ER chaperones are not dynamic, the diffusional mobility of many proteins in the ER becomes restricted, perhaps through the formation of an extensive ER matrix.

Results

Folding characteristics of VSVG–GFP. The conformation-specific anti-VSVG antibody I14 (ref. 15), which detects only correctly folded monomeric and trimeric VSVG molecules, was used to characterize the folding properties of VSVG–GFP. At 40 °C, misfolded VSVG retained in the ER is not recognized by I14, whereas at 32 °C, correctly folded VSVG is present in all intracellular compartments[5,9]. A similar pattern of I14 labelling was observed in COS cells expressing VSVG–GFP (Fig. 1), implying that the thermoreversible folding properties of VSVG were unaffected by the attachment of GFP.

Diffusional mobility of folded and misfolded VSVG–GFP in ER membranes. We used FRAP to compare the diffusional mobilities of folded and misfolded forms of VSVG–GFP in ER membranes. Complete recovery of fluorescence occurred within 5 min of photobleaching of either correctly folded VSVG–GFP at 32 °C in cells treated with brefeldin A (BFA, which prevents the exit of proteins from the ER[16]) or misfolded VSVG–GFP at 40 °C (Fig. 2). In both cases, recovery was rapid and diffusive (the edges of the photobleached box recovered before the centre), and did not involve gross changes in the fine architecture of the ER. This recovery represented the diffusional exchange of unbleached VSVG–GFP for bleached VSVG–GFP, as recovery was abolished when fixed cells were photobleached (data not shown).

Quantitative FRAP analyses showed that folded and misfolded forms of VSVG–GFP, at 32 °C and 40 °C respectively, had indistin-

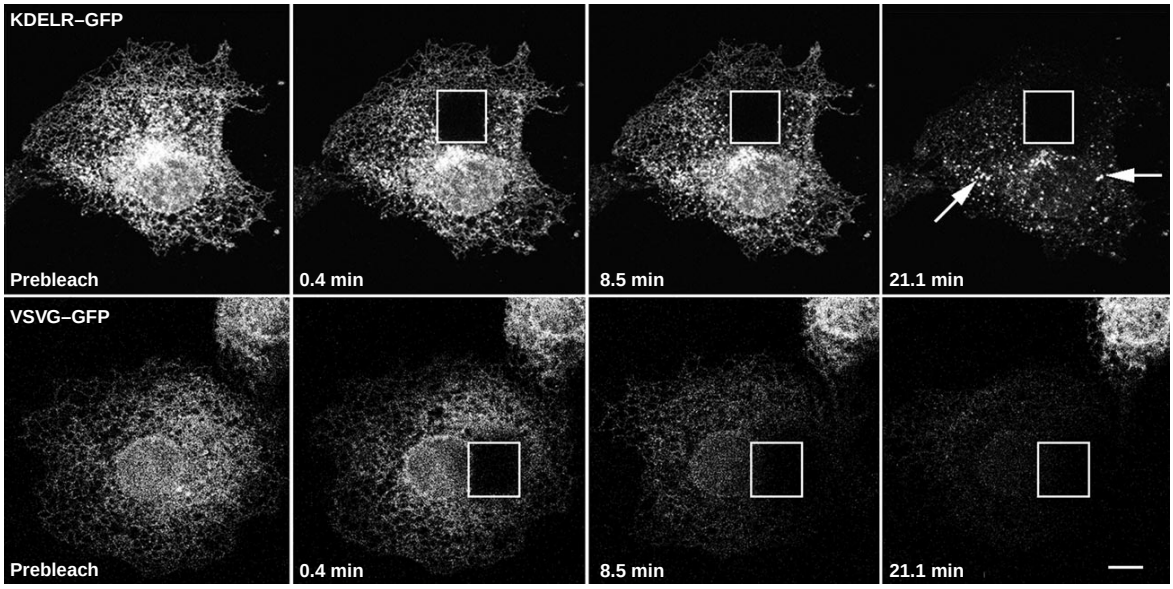

Figure 4 **Repetitive photobleaching of cells expressing KDELR–GFP and VSVG–GFP reveals different mechanisms for their retention in the ER.** A 15 ×15μm box was repeatedly bleached in cells expressing KDELR–GFP (upper panels) or VSVG–GFP (lower panels) at 40°C. Between each bleach, the entire field of view was imaged at low laser power to determine the extent of fluorescence outside the box that was lost as a result of photobleaching within the box. After repeated bleaching, cells expressing KDELR–GFP contain residual fluorescent structures (arrows) and show a loss of ER fluorescence, indicating that recycling of KDELR–GFP back to the ER from pre-Golgi and Golgi structures occurs more slowly than lateral diffusion of KDELR–GFP across the ER lipid bilayer. In contrast, the complete bleaching of the ER and absence of residual fluorescent structures in cells expressing VSVG–GFP indicates that highly mobile, misfolded VSVG–GFP complexes at 40°C never leave the ER. Scale bar represents 10μm.

guishable *D* values (0.4–0.5 $\mu m^2 s^{-1}$) with both forms showing 100% mobility (Fig. 3a, Table 1). *D* values did not vary with the duration of the non-permissive temperature (data not shown), the presence or absence of BFA (Table 1) or the overall level of expression of VSVG–GFP (data not shown). Values for *D* and mobile fraction of VSVG–GFP were comparable to those of other GFP-tagged proteins residing in ER membranes, including lamin-B receptor (LBR), the β-subunit of the signal-recognition-particle receptor (SRβ) and the Golgi enzyme galactosyltransferase (GalT) in cells treated with BFA (Table 1). They were also similar to those of other GFP-tagged proteins present in the Golgi complex[17], all of which had diffusional mobilities at 32°C and 40°C that were close to the theoretical limit for proteins in a lipid bilayer[18,19].

Mechanism of retention of VSVG–GFP in the ER at 40°C. Given that misfolded VSVG–GFP molecules diffuse at a rate close to the viscosity limit in ER membranes, it is clear that these molecules are not retained in the ER at 40°C by mechanisms involving protein immobilization. Two alternative mechanisms of protein retention in the ER are selective retrieval of proteins from post-ER compartments, and failure of proteins to be recognized by ER export machinery. To distinguish between these two models, we repetitively photobleached a 15-μm-square box across the ER while monitoring fluorescence throughout the cell. This allowed us to determine whether VSVG–GFP cycles through separate, discontinuous post-ER structures (as predicted by the retrieval model) or dif-

Table 1 *D* and mobile fraction values for ER-localized GFP chimaeras.

Chimaera	Temp. (°C)	Treatment	*D* ($\mu m^2 s^{-1}$) ± s.d.	M_f ± s.d.	*n*
VSVG–GFP	32	BFA	0.49±0.06	99±4.9	13
VSVG–GFP	40	None	0.45±0.03	102±3.5	23
VSVG–GFP	40	BFA	0.42±0.03	108±3.6	8
LBR–GFP	32	None	0.41±0.10	97±3.9	7
LBR–GFP	40	None	0.50±0.19	93±4.5	9
SRβ–GFP	32	None	0.26±0.03	93±6.4	12
GalT–GFP	32	BFA	0.48±0.03	94±5.5	7
GalT–GFP	40	BFA	0.42±0.06	107±6.6	7

Means ± s.d. of values for *D* and mobile fraction (M_f), for recovery of fluorescence after photobleaching of cells expressing GFP chimaeras under the indicated treatment conditions. Statistical analyses of *D* and M_f values were carried out using a two-tailed student *t*-test. No significant differences were observed for VSVG, LBR or GalT at different temperatures.

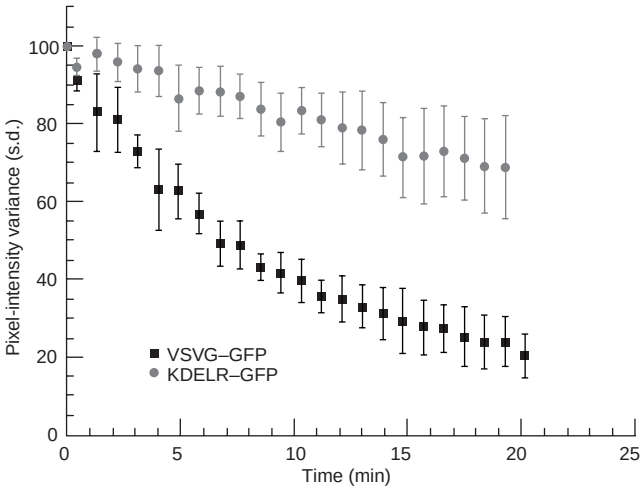

Figure 5 **Cells expressing KDELR–GFP contain more residual fluorescent structures than cells expressing VSVG–GFP after repeated photobleaching.** Pixel-intensity variance (see Methods) in cells expressing VSVG–GFP or KDELR–GFP was plotted against time. Values are means ± s.e.m. from three separate cells. A lower value indicates an increasingly homogeneous population of pixels of similar intensities.

Table 2 Effects of ATP depletion and reducing conditions on the *D* and mobile fraction values of ER-localized GFP chimaeras.

Chimaera	Temp. (°C)	Treatment	*D* ($\mu m^2 s^{-1}$)± s.d.	M_f± s.d.	*n*
VSVG–GFP	40	None	0.45±0.03	102±3.5	23
VSVG–GFP	40	ATP depletion	0.41±0.05	66±5.0*	15
VSVG–GFP	40	ATP depletion then ATP	0.43±0.07	83±2.5*	10
VSVG–GFP	40	ATP depletion + DTT	0.91±0.13*	94±8.3	6
VSVG–GFP	40	BiP(T37G)	0.45±0.21	63.2±13.8*	5
VSVG–GFP	40	WT BiP	0.51±0.10	78±3.3*	6
VSVG–GFP	40	BiP(T37G) + DTT	0.90±0.18*	83±2.7*	6
VSVG–GFP	40	DTT	0.59±0.19	104±8.0	7
GalT–GFP	32	BFA	0.48±0.03	94±5.5	7
GalT–GFP	32	BFA + ATP depletion	0.43±0.07	95±60	11
GalT–GFP	32	BFA + DTT	0.60±0.09	107.3±12.4	6

Means ± s.d. of values for *D* and mobile fraction (M_f), for recovery of fluorescence after photobleaching of cells expressing GFP chimaeras under the indicated treatment conditions. Statistical analyses of *D* and M_f values for different treatments were performed using a two-tailed student *t*-test.

* denotes $P \leq 0.05$ relative to VSVG–GFP or GalT–GFP at 32 °C. DTT, dithiothreitol; WT, wild type.

fuses only within the ER (consistent with the export-defect model). In the retrieval model, repetitive photobleaching would leave pockets of fluorescence corresponding to VSVG–GFP in post-ER compartments, assuming that recycling of VSVG–GFP occurs more slowly than its lateral diffusion across the ER lipid bilayer. This pattern was observed for KDEL receptor tagged with GFP (KDELR–GFP)[17], which rapidly cycles between ER and Golgi membranes (Figs 4, 5; arrows in Fig. 4 denote residual KDELR–GFP fluorescence in post-ER compartments). In the export-defect model, repetitive photobleaching of the ER would remove all fluorescence from the cell, assuming that ER membranes are continuous[20] and that all VSVG–GFP molecules in the ER are mobile. Consistent with this model, we observed uniform loss of VSVG–GFP fluorescence at 40 °C (Figs 4, 5). Retention of VSVG–GFP in the ER at 40 °C thus seems to be a result of failure to efficiently export VSVG-GFP molecules.

Immobilization of VSVG–GFP in ATP-depleted cells. The rapid mobility of misfolded VSVG–GFP at 40 °C suggests that VSVG–chaperone complexes formed at this temperature (including VSVG–BiP and VSVG–calnexin) are either too small to affect the diffusional mobility of VSVG or are highly dynamic (that is, their formation is reversible). In ATP-depleted cells, BiP (an ATP-dependent chaperone)[21] is persistently bound to VSVG[22], leading to interchain crosslinking and aggregation of VSVG[7,8]. In FRAP analyses of cells deprived of ATP for 15–30 min, VSVG–GFP was immobilized at 40 °C (Fig. 3b, Table 2), with no effect on the *D* value of the mobile pool. Immobilization was largely reversed by returning cells to normal (ATP-containing) medium for 20 min (Table 2). ATP depletion had no influence on either the mobile fraction or *D* values of another membrane protein, GalT–GFP, which was localized to the ER using BFA (Table 2). VSVG–GFP was only immobilized in the specialized folding environment of the ER, as there was no change in recovery or mobility of VSVG–GFP during ATP depletion at 32 °C in cells in which VSVG–GFP was localized in the Golgi complex (data not shown).

BiP normally binds to and hydrolyses ATP as it associates and dissociates from proteins[21,22]. We determined whether the immobilization of VSVG–GFP in ATP-depleted cells was a result of the failure of VSVG–GFP to release from BiP in cells expressing an ATPase-inactive BiP mutant, BiP(T37G), which binds to proteins but is unable to release them[23]. In cells examined 24 h after microinjection of plasmid DNA encoding BiP(T37G), a significant fraction

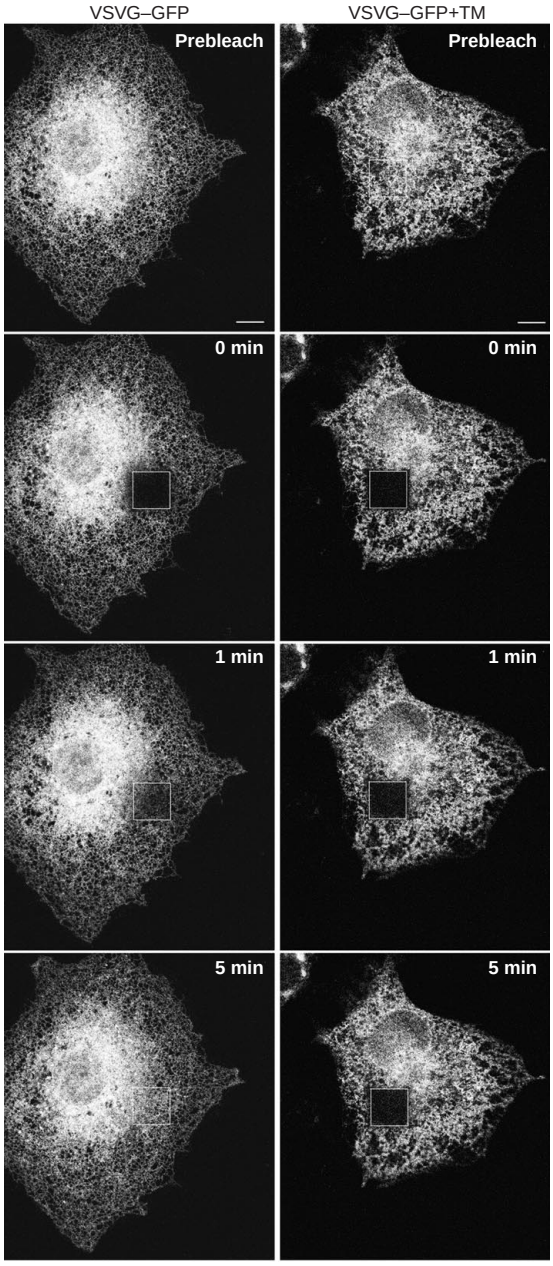

Figure 6 **ER-localized VSVG–GFP is immobilized by tunicamycin treatment.** Qualitative FRAP analysis of ER-localized VSVG–GFP in cells incubated in the absence (left panels) or presence (right panels) of tunicamycin (TM) for 24 h at 40 °C. Images were obtained before photobleaching and at the indicated time points after. The photobleached area is outlined by a box. Scale bars represent 10 μm.

of VSVG–GFP was immobilized, with no change in the overall morphology of the ER (Table 2). VSVG–GFP was also partially immobilized in cells microinjected with cDNA encoding wild-type BiP (Table 2). In contrast, the mobile pool of GalT–GFP (which is not thought to interact with BiP) was not affected by expression of either version of BiP (data not shown). These results indicate that conditions favouring prolonged binding of BiP to substrates, such as expression of a BiP ATPase mutant or overexpression of BiP, lead to immobilization of VSVG–GFP within ER membranes.

VSVG aggregates that form in ATP-depleted cells contain aberrant interchain disulphide bonds[5,7,9] that could potentially contribute to the immobilization of VSVG–GFP observed in our FRAP

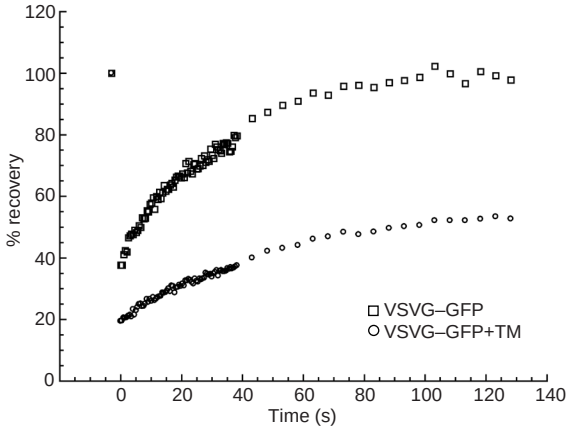

Figure 7 **Immobilization of VSVG–GFP by tunicamycin treatment.** Fluorescence intensities from FRAP analyses were plotted against time for VSVG–GFP in the ER at 40 °C for 24 h in the presence or absence of tunicamycin (TM). Measurements were taken at 0.5-s intervals until a plateau was reached and fluorescence intensities were normalized to prebleach values.

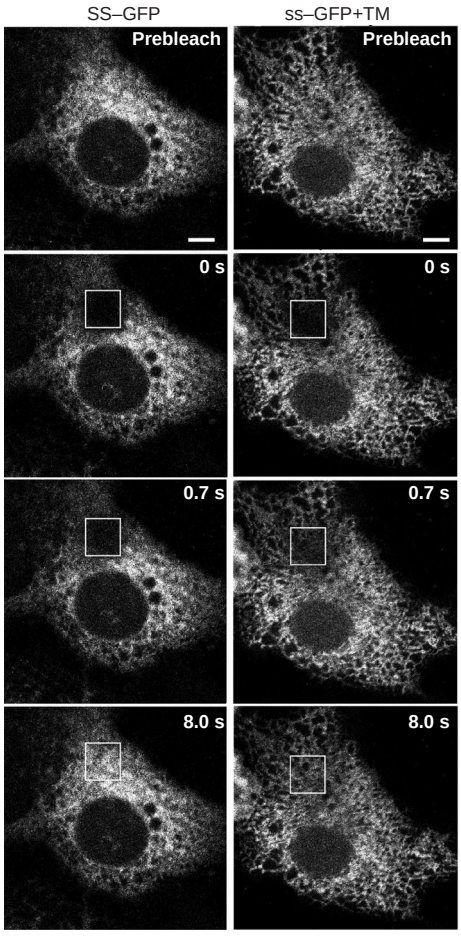

Figure 8 **Diffusional mobility of the soluble ER protein ss–GFP is affected by inhibition of N-linked glycosylation.** Qualitative FRAP analysis of ss–GFP in cells incubated at 40 °C for 24 h in the absence (left panels) or presence (right panels) of tunicamycin (TM). Images were obtained before photobleaching and at the indicated time points after. In tunicamycin-treated cells, partial recovery is evident immediately after photobleaching, in contrast to untreated cells. Scale bars represent 10 μm.

analyses. Within 15 min of the addition of dithiothreitol, which reduces disulphide bonds and inhibits their formation[24,25], to ATP-depleted cells or cells expressing BiP(T37G), immobilization of VSVG–GFP was reversed and *D* was increased by a factor of 2.2 relative to control values (Table 2). Despite their mobilization when treated with dithiothreitol, VSVG–GFP molecules were not recognized by the I14 antibody, implying they were still misfolded (data not shown). These results indicate that the formation of disulphide bonds is important for VSVG–GFP immobilization under conditions of ATP depletion or BiP(T37G) overexpression. Reduction of disulphide bonds had a general effect on the diffusion of membrane proteins in the ER, as the *D* value of GalT–GFP (which contains no intrachain disulphide bonds[17]) localized to the ER using BFA was increased after treatment with dithiothreitol (Table 2).

Immobilization of VSVG–GFP in tunicamycin-treated cells. Sugar moieties are important for increasing the solubility of proteins in the ER to facilitate folding and reduce aggregation[26,27]. VSVG contains two *N*-linked sugar chains and requires these oligosaccharides to fold correctly and be exported from the ER[6–8]. VSVG–GFP was immobilized in cells treated for 24 h at 40 °C with tunicamycin, which blocks the synthesis of dolichol-linked oligosaccharides and thereby inhibits the addition of *N*-linked sugars to proteins (Figs 6, 7). Roughly 50% of VSVG–GFP was immobile in these cells and the *D* value of the mobile pool was reduced by a factor of 1.5 relative to controls (Fig. 7, Table 3). Addition of dithiothreitol to cells treated with tunicamycin did not significantly reverse the immobilization phenotype, although the *D* value of the mobile pool increased under these conditions. It therefore seems that, in the absence of *N*-linked sugars, VSVG-GFP is not freely mobile in ER membranes and undergoes aggregation that cannot be reversed by reducing conditions. Immobilization of proteins by tunicamycin treatment was specific to proteins that are normally glycosylated, as GalT–GFP (which contains no *N*-linked sugars[17]) in cells treated with tunicamycin was only slightly immobilized and its *D* value was increased by a factor of 1.8 relative to controls (Table 3).

Table 3 Effect of tunicamycin treatment on the *D* and mobile fraction values of ER-localized GFP chimaeras.

Chimaera	Temp. (°C)	Treatment	*D* (μm² s⁻¹) ± s.d.	M_f ± s.d.	*n*
VSVG–GFP	40	None	0.45±0.03	102±3.5	23
VSVG–GFP	40	TM	0.30±0.04*	50±2.9*	12
VSVG–GFP	40	TM + DTT	0.47±0.10	60±3.2*	9
GalT–GFP	32	BFA	0.48±0.03	94±5.5	7
GalT–GFP	32	BFA + TM	0.78±0.10*	81±2.2	6

Means ± s.d. of values for *D* and mobile fraction (M_f), for recovery of fluorescence after photobleaching of cells expressing GFP chimaeras under the indicated treatment conditions. Statistical analyses of *D* and M_f values for different treatments were carried out using a two-tailed student *t*-test.

* denotes $P \leq 0.05$ relative to VSVG–GFP at 40 °C or GalT–GFP at 32 °C. TM, tunicamycin; DTT, dithiothreitol.

Effect of ATP depletion and tunicamycin on the ER lumenal environment. The changes in diffusional mobility of VSVG–GFP localized to the ER, involving disruption of protein-folding pathways, led us to ask how the overall ER environment is affected under these conditions. To address this question, we used a soluble probe targeted to the ER lumen, comprising GFP carrying an ER signal sequence (ss–GFP). In untreated cells, ss–GFP diffused significantly faster than proteins embedded in ER membranes, completely recovering into a photobleached box within 8 s of photobleaching (Fig. 8). ATP depletion resulted in slower diffusion of ss–GFP in the ER than in control cells as well as a decrease in its mobile fraction value (Fig. 9a, b). The effect of ATP depletion was reversed upon the return of cells to normal medium (data not shown), but was unaffected by

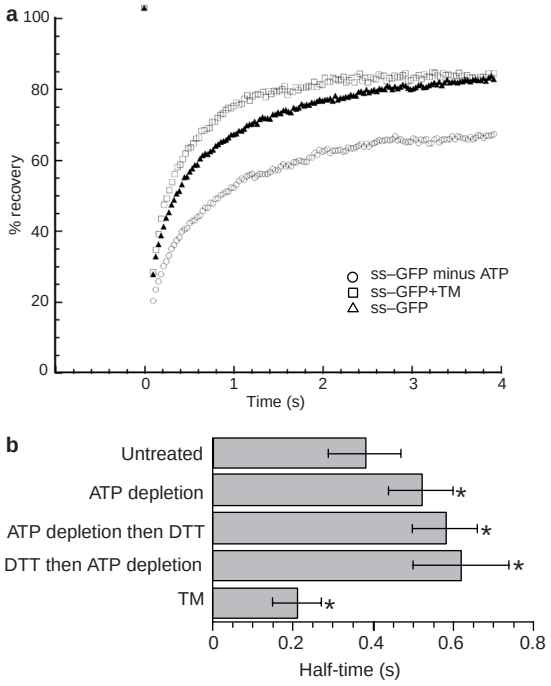

Figure 9 **Effects of ATP depletion, tunicamycin and dithiothreitol on mobility of ss–GFP. a**, Fluorescence intensities from quantitative FRAP analyses were plotted against time for ss–GFP in the ER at 40 °C with no treatment, after 24 h of tunicamycin (TM) treatment, or after 15 min of ATP depletion. **b**, Half-time values for recovery of fluorescence after photobleaching of cells expressing ss–GFP in the ER lumen subjected to the indicated treatments (see Methods). Lower values indicate faster recoveries. Values are means from at least six cells. Values for the different treatment conditions were compared to those from untreated cells using a two-tailed student *t*-test. * denotes $P \leq 0.01$; DTT, dithiothreitol.

incubation of cells with dithiothreitol, either before or during ATP depletion (Fig. 9b). In contrast, ss–GFP diffused significantly faster in cells treated with tunicamycin than in untreated cells (Figs 8, 9a, b). These results indicate that whereas energy depletion may cause lumenal proteins to diffuse more slowly, possibly because of extensive crosslinking of BiP-containing protein aggregates within the ER lumen, tunicamycin treatment may markedly increase their mobility. As ss–GFP does not contain sugar moieties, these results indicate that *N*-linked sugars on ER glycoproteins may be important in determining the viscous properties of the ER lumen. Without such sugar moieties, the ER lumen seems to be less viscous.

Discussion

We have shown that VSVG–GFP diffuses freely and rapidly throughout the ER when properly folded at 32 °C or misfolded at 40 °C. This implies that misfolded VSVG–GFP complexes at 40 °C are not impeded by lumenal or cytoplasmic interactions, or restricted diffusion through a matrix. What then explains the ER-retention phenotype of these molecules at 40 °C? Although selective retrieval from post-ER compartments underlies the ER localization of several membrane proteins including ERGIC-53, p58 and KDELR[28–30], our data indicate that VSVG–GFP may be retained in the ER by a different mechanism. Repetitive photobleaching of a small area in the ER containing VSVG–GFP at 40 °C eliminated cellular fluorescence (including the nuclear envelope) with no pockets of fluorescence remaining. This contrasts with results for cells expressing the rapidly recycling molecule KDELR–GFP, in which an identical bleaching protocol left pockets of fluorescence representing KDELR–GFP molecules that had not yet recycled back to the ER. These results indicate that misfolded VSVG–GFP complexes may be retained in the ER at 40 °C either by failing to be released from dynamically interacting folding factors or by failing to be recognized by ER export machinery.

At 40 °C the association of misfolded VSVG with ER chaperones, including BiP and calnexin, is enhanced[6–8]. Why is there no difference in the diffusional mobility of these complexes and of correctly folded VSVG–GFP complexes in the ER at 32 °C? The most likely explanations are that VSVG–chaperone complexes that form at 40 °C are either too small to affect the diffusional mobility of VSVG, or that the formation of these complexes is highly reversible. The apparent *D* values (0.4–0.5 $\mu m^2 s^{-1}$) for misfolded and correctly folded VSVG–GFP complexes in the ER, at 40 °C and 32 °C respectively, were similar to those for other ER localized membrane proteins, including GalT, SRβ, LBR (Table 1), and major histocompatibility complex (MHC) class I proteins[31], all of which have diffusional mobilities close to the theoretical limit for proteins in a lipid bilayer. They are higher than the *D* values reported for ER-localized TAP[31] and cytochrome P450 (ref. 32). The lower *D* value for TAP may reflect the large size of TAP complexes, which are involved in peptide loading of MHC class I proteins[33]. These complexes have an estimated diatmeter of 600–1,000 Å and are thought to consist of hundreds of molecules[31]. The rate of lateral diffusion of a protein embedded in a bilayer is proportional to the logarithm of the radius of the diffusing molecule, so VSVG–GFP complexes (which have a twofold higher *D* value than TAP) must be at least an order of magnitude smaller than TAP complexes.

When we prevented VSVG from dissociating from chaperones through ATP depletion, which causes interchain crosslinking and aggregation of VSVG complexes[7], a significant pool of VSVG–GFP molecules became immobilized. There are several possible explanations for this. The VSVG aggregates could be of variable size and some may therefore be too big to diffuse. Alternatively, mobile VSVG–GFP aggregates may form a crosslinked network in which boundaries in some areas become closed, preventing diffusion of other VSVG–GFP aggregates across the area. However, this would be expected to result in entrapment of other membrane proteins and our data showed no effect of ATP depletion on the *D* or mobile fraction values for ER-localized GalT–GFP. A third possibility is that ATP depletion leads to the association of VSVG with other proteins, including BiP, calnexin and PDI, and their interacting substrates, which are either already relatively immobile in the ER or become immobile under ATP depletion by crosslinking into a scaffold.

To explore the third possibility we investigated the function of BiP, an ATP-dependent chaperone that forms complexes with VSVG at 40 °C[5,7], in the immobilization of VSVG–GFP during ATP depletion. ATP depletion causes BiP to bind persistently to VSVG as well as to other substrates[5,7,22]. This may explain why VSVG–GFP is immobilized in ATP-depleted cells, as prolonged BiP binding may cause VSVG to be present in a more extended conformation, allowing crosslinking with other proteins. This idea is supported by our finding that conditions, other than ATP depletion, that favour prolonged binding of BiP to substrates, including expression of a BiP ATPase mutant and overexpression of BiP, also lead to immobilization of VSVG–GFP molecules in the ER.

Interchain disulphide bonds within VSVG aggregates, which form in ATP-depleted cells[7,13], are necessary to immobilize VSVG–GFP in ATP-depleted cells, as reduction of these disulphide bonds through treatment with dithiothreitol reversed the immobilization caused by either ATP depletion or overexpression of the BiP mutant. Dithiothreitol treatment alone increased the diffusion coefficient of GalT–GFP (which does not contain disulphide bonds) in ER membranes. This may reflect a general effect of the reduction of disulphide bonds on membrane viscosity, or a more direct effect of proteins no longer associating in dynamic crosslinked aggregates.

We found that treatment of cells with tunicamycin also inhibits the diffusional mobility of VSVG–GFP. The immobile pool under these conditions may result from the formation of large aggregates

of misfolded VSVG, as *N*-linked sugars have an important function in the folding pathways of VSVG and of other proteins in the ER[26,27]. If so, these aggregates would seem to be distinct from VSVG–GFP aggregates formed in ATP-depleted cells, as treatment with dithiothreitol reversed the immobilization phenotype in ATP-depleted but not tunicamycin-treated cells. The observed increase in the *D* value of GalT–GFP, which is not known to be a substrate of BiP or to contain *N*-linked sugars, during tunicamycin treatment may be a result of a less crowded lumenal environment, caused either by enhanced aggregation of normally *N*-glycosylated proteins or by the absence of carbohydrate side chains on glycoproteins. The small immobile pool of GalT–GFP under these conditions may result from GalT–GFP being trapped in networks of immobile protein aggregates.

To investigate how the ER lumenal environment, which is thought to be a viscous gelatinous mass without internal structure[34], is affected by ATP depletion and tunicamycin treatment, we measured the diffusional mobility of a soluble ER protein, ss–GFP, under these conditions. In untreated cells, the half-time for recovery of ss–GFP into a photobleached box was extremely rapid, many times faster than that for recovery of VSVG–GFP into a box of similar size. This indicates that movement in the ER lumenal space may normally be unrestricted, and is consistent with the previous finding that the rate of diffusion of KDEL–GFP in the ER lumen is slightly lower than that of cytoplasmic solutes[20]. However, when the association of chaperones with ER proteins is enhanced by ATP depletion or blocking of oligosaccharide addition onto glycoproteins by tunicamycin treatment, there are concomitant global effects on the ER lumenal environment.

Whereas ATP depletion caused ss–GFP to diffuse more slowly, tunicamycin treatment caused it to diffuse much more quickly. Our results from tunicamycin treatment indicate that the presence of oligosaccharide side chains on proteins may be an important factor in determining the lumenal viscosity of the ER. Branched oligosaccharides on proteins are large (roughly 20 Å in length) and extend through volumes of ~104 $Å^3$ (refs 12, 35). They are therefore likely to occupy a significant volume of the ER lumen and to restrict diffusion through their polymer network. This is supported by our finding that proteins diffuse much faster when oligosaccharides are absent from proteins in tunicamycin-treated cells.

Diffusion of ss–GFP is slowed in ATP-depleted cells. This indicates that the ER lumen may be dynamic and capable of forming a dense protein mesh, which impedes the diffusion of soluble ER proteins, when chaperone–protein interactions are promoted. This matrix may be composed of the lumenal moieties of membrane proteins such as VSVG, which, through prolonged binding to BiP, may form aberrant crosslinks with proteins that extend deep into the ER lumen. Further study is needed to understand the regulation of such an ER lumenal matrix, including how its density is controlled so that soluble markers change their mobility. The quantitative methods described here for determining the mobility of proteins in the ER may be useful in answering these questions. They may also be important in investigating further the ER characteristics that underlie the quality-control functions of protein folding and maturation[36,37] and protein-unfolding responses[38]. □

Methods

Cell lines, antibodies and reagents.

COS-7 cells were grown in DMEM (Biofluids, Rockville, MD) supplemented with 10% fetal bovine serum (FBS), 2 mM glutamine, 100 U ml^{-1} penicillin and 100 µg ml^{-1} streptomycin at 37 °C in a 5% CO_2 incubator and were used in all experiments. I14 [1E9F9] antibodies were kindly provided by D. Lyles (Wake Forest University, Winston-Salem, NC). BFA (Epicentre Technologies, Madison, WI) was used at 5 µg ml^{-1}. Cellular ATP levels were depleted using 50 mM 2-deoxy-glucose and 0.02% sodium azide in glucose-free medium. Tunicamycin (Sigma) was used at 5 µg ml^{-1} for 24 h to block addition of oligosaccharide chains to proteins, and dithiothreitol (Sigma) was used at 5 mM for 15 min to reduce disulphide bonds. cDNA (**AU: OK?**) plasmids encoding BiP and BiP(T37G) were kindly provided by L. Hendershot (University of Tennessee Medical Center, Memphis, TN).

Construction and expression of GFP chimaeras.

Cloning and expression of VSVG–GFP, LBR–GFP, GalT–GFP and KDELR–GFP were carried out as described[3,17,39]. The SRβ–GFP construct comprises the mouse cDNA for SRβ fused to the GFP(S65T) variant in the mammalian expression vector pcDNA1.1 (Invitrogen). The ss–GFP construct, cloned into the mammalian expression vector pCDM8, encodes the first 19 amino acids of hen egg lysozyme fused to GFP, omitting its initiation methionine residue. Cells were transfected with chimaeric DNA by electroporation as described[17], typically incubated at 37 °C for 24 h and then transferred to 40 °C or 32 °C in BFA as indicated. Alternatively, cells at 80–90% confluence in 6-well plates were transfected with 1 µg plasmid DNA with FuGENE6 transfection reagent (Boehringer) and incubated at 40 °C. For the effect of BiP(T37G) expression, cells expressing VSVG–GFP were microinjected with 2 mg ml^{-1} plasmid DNA and 2 mg ml^{-1} rhodamine dextran for identification of injected cells. Cells were fixed in 2% formaldehyde and stained with I14 antibodies as described[16].

FRAP analyses.

Analyses were performed on a temperature-controlled stage of a Zeiss LSM410 confocal microscope, using the 488-nm line of a 400-mW Ar/Kr laser with a 100×, 1.4 NA objective. A defined region (outlined box in figures) was photobleached at full laser power (100% power, 100% transmission, 30 s); recovery of fluorescence was monitored by scanning the whole cell at low laser power (30% power, 0.3% transmission). No photobleaching was observed during recovery.

Quantitative diffusion measurements, for generating recovery plots, and *D* values were obtained by photobleaching the entire depth of a 4-µm-wide strip extending across cell borders as described[17]. Repetitive photobleaching experiments were carried out at 40 °C on the temperature-controlled stage of a Zeiss LSM410 confocal microscope as described[17].

To quantify the presence of residual fluorescent structures in cells subjected to repetitive photobleaching (Fig. 5), standard deviations of pixel intensity within a 15 µm×15 µm area were measured using NIH Image 1.62, in which one pixel represents 0.25 µm×0.25 µm. A larger s.d. corresponds to a wider range of pixel-intensities. Thus, an area containing both bright structures and dim surrounding pixels would have a large s.d. Conversely, a smaller s.d. corresponds to a relatively homogenous population of pixels of similar intensities. Values were normalized for each FLIP series by dividing by the s.d. at time zero (prebleach) for each cell and multiplying by 100. This process was carried out for three cells expressing KDELR–GFP and three cells expressing VSVG–GFP. Means ± s.e.m. for the three cells at each time point were plotted. The area evaluated did not include the Golgi, nucleus, or bleached box.

Recovery of the ss–GFP chimera was too fast to measure accurately using the Zeiss LSM410 confocal microscope. Quantitative FRAP measurements for this protein were therefore made using a Zeiss 510 confocal microscope with a 40×, 1.3 NA objective. We compared relative recovery rates for ss–GFP using the half-time for recovery of fluorescence towards the asymptote. As for *D*-value calculations, time was corrected by setting time zero as equal to the half-time of the bleach. Qualitative FRAP analyses were carried out by photobleaching a defined region (outlined box in Figs) at full laser power (100% power, 100% transmission) and then monitoring recovery of fluorescence by scanning the defined region at low laser power (100% power, 0.3% transmission).

For all quantitative FRAP analyses, values for *D*, half-time and mobile fraction were compared with control conditions for each chimaera for significance using a two-tailed student *t*-test. Values of $P < 0.05$ were considered significant.

RECEIVED 9 SEPTEMBER 1999; REVISED 9 FEBRUARY 2000; ACCEPTED 16 MARCH 2000; PUBLISHED 7 APRIL 2000.

1. Kreis, T. E. & Lodish, H. F. Oligomerization is essential for transport of vesicular stomatitis viral glycoproteins to the cell surface. *Cell* **46,** 929–937 (1986).
2. Bergmann, J. E. Using temperature-sensitive mutants of VSV to study membrane protein biogenesis. *Methods Cell Biol.* 32, 85–110 (1989).
3. Presley, J. F. *et al.* ER-to-Golgi transport visualized in living cells. *Nature* **389,** 81–85 (1997).
4. Doms, R. W., Keller, D. S., Helenius, A. & Balch, W. E. Role of adenosine triphosphate in regulating the assembly and transport of vesicular stomatitis virus G protein trimers. *J. Cell Biol.* **105,** 1957–1969 (1987).
5. Machamer, C. E., Doms, R. W., Bole, D. G., Helenius, A. & Rose, J. K. Heavy chain binding protein recognizes incompletely disulfide-bonded forms of vesicular stomatitis virus G protein. *J. Biol. Chem.* **265,** 6879–6883 (1990).
6. De Silva, A., Balch, W. E. & Helenius, A. Quality control in the endoplasmic reticulum: folding and misfolding of vesicular stomatitis virus G protein in cells and in vitro. *J. Cell Biol.* **111,** 857–866 (1990).
7. De Silva, A., Braakman, I. & Helenius, A. Post-translational folding of vesicular stomatitis virus G protein in the ER: involvement of noncovalent and covalent complexes. *J. Cell Biol.* **120,** 647–655 (1993).
8. Hammond, C. & Helenius, A. Folding of VSVG protein: sequential interaction with BiP and calnexin. *Science* **266,** 456–458 (1994).
9. Doms, R. W., Ruusala, A., Machamer, C., Helenius, A. & Rose, J. K. Differential effects of mutations in three domains on folding, quaternary structure, and intracellular transport of vesicular stomatitis virus G protein. *J. Cell Biol.* **107,** 89–99 (1988).
10. Hammond, C. & Helenius, A. Quality control in the secretory pathway. *Curr. Opin. Cell Biol.* **7,** 525–539 (1995).
11. Hammond, C. & Helenius, A. Quality control in the secretory pathway: retention of a misfolded viral membrane glycoprotein involves cycling between the ER, intermediate compartment and Golgi apparatus. *J. Cell Biol.* **126,** 41–52 (1994).
12. Edidin, M. in *Mobility and Proximity in Biological Membranes* (eds Damjanovich, S., Edidin, M., Szollosi, J & Tron, L.) 109–135 (CRC, Boca Raton, Florida, 1994).
13. Braakman, I., Helenius, J. & Helenius, A. Role of ATP and disulphide bonds during protein folding in the endoplasmic reticulum. *Nature* **356,** 260–262 (1992).
14. Leavitt, R., Schlessinger, S. & Kornfeld, S. Impaired intracellular migration and altered solubility of nonglycosylated glycoproteins of vesicular stomatitis virus and Sindbis virus. *J. Biol. Chem.* **252,** 9018–9023 (1977).
15. Lefrancois, L. & Lyles, D. S. The interaction of antibody with the major surface glycoprotein of vesicular stomatitis virus. I. Analysis of neutralizing epitopes with monoclonal antibodies. *Virology* **121,** 157–166 (1982).

16. Lippincott-Schwartz, J. *et al.* Microtubule-dependent retrograde transport of proteins into the ER in the presence of brefeldin A suggests an ER recycling pathway. *Cell* **60,** 821–836 (1990).
17. Cole, N. B. *et al.* Diffusional mobility of Golgi proteins in membranes of living cells. *Science* **273,** 797–801 (1996).
18. Poo, M., & Cone, R. A. Lateral diffusion of rhodopsin in the photoreceptor membrane. *Nature* **247,** 438–441 (1974).
19. Hughes, B. D., Pailthorpe, B. A., White, L. R. & Sawyer, W. H. Extraction of membrane microviscosity from translation and rotational diffusion coefficients. *Biophys. J.* **37,** 673–676 (1982).
20. Dayel, M. J., Hom, E. F. Y. & Verkman, A. S. Diffusion of green fluorescent protein in the aqueous-phase lumen of endoplasmic reticulum. *Biophysical J.* **76,** 2843–2851 (1999).
21. Kassenbrock, C. K. & Kelly, R. B. Interaction of heavy chain binding protein (BiP/GRP78) with adenine nucleotides. *EMBO J.* **8,** 1461–1467 (1989).
22. Dorner, A. J., Wasley, L. C. & Kaufman, R. J. Protein dissociation from GRP78 and secretion are blocked by depletion of cellular ATP levels. *Proc. Natl Acad. Sci. USA* **87,** 7429–7432 (1990).
23. Hendershot, L.M. *et al. In vivo* expression of mammalian BiP ATPase mutants causes disruption of the endoplasmic reticulum. *Mol. Biol. Cell* **6,** 283–296 (1995).
24. Braakman, I., Helenius, J. & Helenius, A. Manipulating disulfide bond formation and protein folding in the endoplasmic reticulum. *EMBO J.* **11,** 1717–1722 (1992).
25. Tatu, U., Braakman, I. & Helenius, A. Membrane glycoprotein folding, oligomerization and intracellular transport: effects of dithiothreitol in living cells. *EMBO J.* **12,** 2151–2157 (1993).
26. Helenius, A. How *N*-linked oligosaccharides affect glycoprotein folding in the endoplasmic reticulum. *Mol. Biol. Cell* **5,** 253–265 (1994).
27. Helenius, A., Trombetta, E. S., Hebert, D. N. & Simons, J. F. Calnexin, calreticulin and the folding of glycoproteins. *Trends Cell Biol.* **7,** 193–201 (1997).
28. Saraste, J. & Kuismanen, E. Pathways of protein sorting and membrane traffic between the rough endoplasmic reticulum and the Golgi complex. *Semin. Cell Biol.* **3,** 343–355 (1992).
29. Schweizer, A. *et al.* Identification of an intermediate compartment involved in protein transport from endoplasmic reticulum to Golgi apparatus. *Eur. J. Cell Biol.* **53,** 185–196 (1990).
30. Lewis, M. J. & Pelham, H. R. Ligand induced redistribution of a human KDEL receptor from the Golgi complex to the endoplasmic reticulum. *Cell* **68,** 353–364 (1992).
31. Marguet, D. *et al.* Lateral diffusion of GFP-tagged $H2L^d$ molecules and of GFP–TAP1 reports on the assembly and retention of these molecules in the endoplasmic reticulum. *Immunity* **11,** 231–240 (1999).
32. Szcesna-Skorupa, E., Chen, C. D., Rogers, S. & Kemper, B. Mobility of cytochrome P450 in the endoplasmic reticulum membrane. *Proc. Natl Acad. Sci. USA* **95,** 14793–14798 (1998).
33. Howard, J. C. Supply and transport of peptides presented by class I MHC molecules. *Curr. Opin. Immunol.* **7,** 69–76 (1995).
34. Koch, G. L. E. Reticuloplasmins: a novel group of proteins in the endoplasmic reticulum. *J. Cell Sci.* **87,** 491–492 (1987).
35. Wier, M. & Edidin, M. Constraint of the translational diffusion of a membrane glycoprotein by its external domains. *Science* **242,** 412–414 (1988).
36. Helenius, A., Marquardt, T. & Braakman, I. The endoplasmic reticulum as a protein-folding compartment. *Trends Cell Biol.* **2,** 227–231 (1992).
37. Hurtley, S. M. & Helenius, A. Protein oligomerization in the endoplasmic reticulum. *Annu. Rev. Cell Biol.* **5,** 277–307(1989).
38. Sidrauski, C., Chapman, R. & Walter, P. The unfolded protein response: an intracellular signalling pathway with many surprising features. *Trends Cell Biol.* **8,** 245–249 (1998).
39. Ellenberg, J. *et al.* Nuclear membrane dynamics and reassembly in living cells: targeting of an inner nuclear membrane protein in interphase and mitosis. *J. Cell Biol.* **138,** 1193–1206 (1997).

ACKNOWLEDGEMENTS

We thank B. Nichols, K. Hirschberg and J. Bonifacino for comments and suggestions and P. Walter (USCF, San Francisco, CA) for SRβ DNA. E.S. is supported by a grant (ROI GM59018-01) from the NIH. Correspondence and requests for materials should be addressed to J.L-S.

